# New Results on the Continuous Cooling Behaviour of an ASTM A335 P92 Steel

M.N. Xaubet[1], C.P.Ramos[2], C.A. Danón[3]

[1]Physics Department, Faculty of Exact and Natural Sciences, Buenos Aires University, Buenos Aires, Argentina

[2]National Atomic Energy Commission, Research and Applications Department, Buenos Aires, Argentina

[3]National Atomic Energy Commission, Materials Department, Buenos Aires, Argentina

*E-mail contact of main author: danon@cnea.gov.ar*

**Abstract.** This work introduces new results on the transformation behavior and microstructural evolution of ASTM A335 P92 steel under continuous cooling conditions (CCT). The first results were already reported and stored in the INIS database under the report number INIS-AR-C--1704.

The material was austenized at 1050 ºC and afterwards cooled down at controlled rates (300, 200, 140, 120, 100, 90, 70, 50, 25 and 15 ºC/h). The transformation behavior of the steel samples was followed by dilatometry.

The determination of the phases present in the samples after the thermal cycles was performed by optical and field emission scanning electron microscopy for the eleven tested values of cooling rate. Additionally, a full characterization was performed for selected samples by Mössbauer spectroscopy and X-ray diffraction.

The phase domains identified according to the cooling rate were completely martensitic, completely ferritic and mixed martensitic-ferritic. Second-phase precipitation has been observed in all of the samples, and indications of the presence of retained austenite after some of the cooling cycles were also detected. The experimental results were collected in the form of a continuous cooling transformation diagram.

**Key Words**: P92 steel, phase transformation, retained austenite, Mössbauer spectroscopy.

## 1. Introduction

Ferritic-martensitic steels of the 9%Cr1%Mo type have been extensively used in conventional power plant components, heat exchangers, piping and tubing, etc., due to an excellent combination of properties such as creep resistance, toughness and resistance to oxidation at high temperatures. In the four last decades, 9%Cr1%Mo-based, modified alloys have also been designed and studied for applications as structural materials in the new generation of nuclear fission reactors, which will work at high to very high temperatures (Generation IV reactors) and fusion reactors as well. These new applications have raised very exigent requirements to be fulfilled, as the high temperature and aggressive environment standard service conditions must now be coupled with the existence of strong irradiation fields.

The standard microstructure after normalizing at 1050-1060 ºC and tempering at 750-760 ºC is a lath martensite, and the main types of precipitates after this sequence are $M_{23}C_6$ carbides (M=Cr, Fe) and MX carbonitrides (M=Nb,V; X= C,N).

The Continuous Cooling Transformation (CCT) diagrams of 9%Cr steels are relatively simple and display basically three phase fields, i.e., austenite, ferrite and martensite, with the added presence of carbides in all of them [1,2,3]. The key features of the CCT diagram of P/T91 steels

include two critical cooling rate values: $c_\alpha$, which represents the maximum cooling rate to achieve a fully ferritic microstructure, and $c_m$, which amounts the minimum cooling rate to find a fully martensitic microstructure. For cooling rates between these two values, the final microstructure is a mix of martensite and ferrite (with precipitated carbides). The martensite start temperature $M_s$ remains relatively uniform (~380-400 ºC) within a broad interval of cooling rates in the martensitic domain, and then shows a distinct increase in the mixed domain. On the other hand, bainite has never been reported to form as a result of continuous cooling in 9%Cr steels.

Having the main focus of attention as for cooling behaviour studies traditionally been directed towards welding or normalizing conditions, the literature on the characterization of the metallurgical state of 9%Cr steels after continuous cooling at slow to moderate rates is scarce. Despite the good knowledge of the CCT diagram of these alloys, some issues still deserve a renewed attention. Novel ideas have been proposed expected to be potentially useful in designing new heat treatments of these steels, which include the introduction of a non-vanishing ferrite fraction in the final product via isothermal steps or cooling at moderate to slow rates [4,5], and merit a revision of the less-explored region of the CCT diagram. Another application case pointing out the relevance of microstructural studies on slow continuous cooling comes from manufacture processes of thick-walled components. As the wall becomes thicker, the cooling rate of the central section slows down; as a result, martensite domains or ferrite grain size (if any) may coarse and the precipitation conditions may change [6].

In this contribution, the microstructure of samples tested under continuous cooling conditions in a broad range of cooling rates is studied and characterized by several techniques; in particular, as for the presence of cementite and retained austenite.

## 2. Material and Methods

The chemical composition of the starting material (grade P92 steel) is shown in Table 1.

TABLE I: CHEMICAL COMPOSITION OF THE ASTM A335 P92 STEEL (WT. %).

| **Elem.** | C | Si | Mn | Cr | Mo | Ni | Al | Nb | V | N | B | W | Fe |
|---|---|---|---|---|---|---|---|---|---|---|---|---|---|
| **Wt. %** | 0.13 | 0.24 | 0.46 | 8.72 | 0.38 | 0.17 | 0.01 | 0.06 | 0.2 | 0.05 | 0.002 | 1.63 | Bal. |

Specimens were rectangular prisms 25 x 6 x 6 $mm^3$, machined in the rolling direction from a tube with 73 mm in internal diameter and 9.53 mm in wall thickness. Heat treatments were done in a high temperature dilatometer Adamel DHT 60 under vacuum better than $10^{-5}$ Torr. Thermal cycles were as follows: heating at 300 ºC/h up to 1050 ºC (i.e., to the austenite phase field), holding at 1050 ºC for 30 min and then cooling at controlling rates of 300, 200, 140, 120, 110, 100, 90, 70, 50, 25 and 15 ºC/h.

A subset of selected dilatometer-tested samples, as well as a specimen in the as-received metallurgical state, were fully characterized by Optical Microscopy (OM), Field Emission Gun Scanning Electron Microscopy (FEG-SEM), X-Ray Diffraction (XRD) and Mössbauer Spectroscopy (MS). Samples were longitudinally cut so as to expose the mid plane, and the surface of that plane was prepared by the standard metallographic procedures for examination. Chemical etching was done with the Villela or Nital reagents, depending on the microstructure expected to be revealed.

The ferrite fraction in "mixed" (i.e. martensitic-ferritic) samples was estimated from OM, using 15 fields 280 x 210 $\mu m^2$ at a working magnification of 500 X, by means of a commercial software for image analysis. Microstructures were also observed at high resolution in a Zeiss Supra 40 FEG-SEM operated at 5 keV accelerating voltage. XRD measurements were done in a Panalytical Empyrean diffractometer, using the $\theta$-$2\theta$ Bragg-Brentano geometry, a flat graphite monochromator and Ni-filtered Cu-K$\alpha$ radiation. The spectra were processed by the Rietveld refinement method with the software MAUD (Materials Analysis Using Diffraction) [7].

### 2.1.XRD Pattern Refinement and Treatment of Martensite-Ferrite Overlapping

The matrix was considered to be either bct martensite (space group: I4 mmm) or bcc ferrite (space group: Im-3m), or a mixed martensite-ferrite one. This assumption was made in each case based on previous microscopic observations, as explained in Section 3. The software allows for an analysis of the peak broadening arising from physical effects such as diffraction domain size and microstrains; even in cases where there is size and strain anisotropy resulting in profiles with different Miller indices which are broadened in a different way. The crystallite size and the microstrain were evaluated using the Popa model [8]. In order to obtain the Caglioti function [9] giving the instrumental broadening a Si standard was measured in the same experimental conditions.

On the other hand, the experimental intensities of the different peaks of the matrix (either bct or bcc) were observed to be slightly different from the simulated ones for the case of a random polycrystalline sample and thus they had to be corrected by applying an arbitrary texture factor for each reflection [10].

The mixed martensitic-ferritic microstructures in low carbon steels display XRD peaks practically indistinguishable as for their angular position. However, martensite has a highly deformed microstructure that produces broadening of their diffraction peaks, giving a chance to attempt to a separation from the ferrite ones (which are much narrower) through the assumption of different widths for the peaks of each phase.

Thanks to the above mentioned software features, broadening could be modeled for the martensite phase and reduced or discarded for ferrite. Nevertheless, given the large number of parameters involved in the refinement and the overlapping of peak positions, some initial constraints are unavoidable in order to obtain a stable final result for the refinement. Thus, the initial values for the martensite lattice parameters were linked to the ferrite one so as to have

$a_M = a_F - 0.001$ [Å]

$c_M = a_F + 0.001$ [Å],

where M and F denote martensite and ferrite respectively. In the first refinement cycles, only $a_F$ was considered as a refinable parameter and texture corrections were excluded from calculations. Once the general fit and the calculated phase fractions were observed to keep approximately steady as a function of the number of iterations, the martensite lattice parameters were released and texture factors were allowed, to arrive to the final result. Even so, the calculated volume fractions should be judged cautiously, as the solution found is far from being unique (for instance, if the initial constraints are changed).

### 2.2.Mössbauer Spectroscopy

Measurements were performed at room temperature (RT) in the transmission geometry with a conventional Mössbauer spectrometer set in constant acceleration mode with a $^{57}$Co source in a Rh matrix. Spectra were recorded on powdered samples at 11 mm/sec and fitted by using the Normos program developed by Brand [11], according to two different procedures; i.e., by

decomposition in broadened discrete sextets with a least-squares fit to Lorentzian lines and then by using hyperfine field distributions. Decomposition was made considering six subspectra. Five of them (sextets 1 to 5) model the different surroundings of Fe atoms in the bcc matrix, i.e. Fe atoms with different number of substitutional close neighbors. The sixth subspectrum (sextet 6) would correspond to precipitates of the alloyed cementite phase ($(Fe,Cr)_3C$). Isomer shift (IS) values are given relative to that of α-Fe at RT.

## 3. Results and Discussion

### 3.1.Dilatometry and Optical Microscopy

Matrix phase transformations occurred during cooling were detected on the grounds of the dilation signal. Transformation temperatures measured from the dilation curves are presented in Table 2. Asterisks indicate that the final microstructure contains martensite (*) or ferrite (**), but the corresponding phase transformations couldn't be identified by dilatometry.

TABLE 2: START AND FINISH TEMPERATURES FOR THE MARTENSITIC (TM) AND FERRITIC (TF) TRANSFORMATIONS, AS EXTRACTED FROM DILATOMETRIC CURVES (TEMPERATURE UNCERTAINTY: ± 5 ºC).

| **Cooling rate (ºC/h)** | **TM (ºC)** | | **TF (ºC)** | |
|---|---|---|---|---|
| | Start (Ms) | end | start | end |
| 300 | 336 | 160 | | |
| 200 | 343 | 166 | | |
| 140 | 345 | 151 | ** | |
| 120 | 349 | 151 | ** | |
| 110 | 344 | 153 | ** | |
| 100 | 358 | 155 | ** | |
| 90 | 360 | 177 | ** | |
| 70 | 369 | 200 | 735 | 638 |
| 50 | 412 | 234 | 724 | 642 |
| 25 | * | | 749 | 651 |
| 15 | | | 759 | 688 |

OM observations representative of the three different cooling rate domains are as follows:

i. The specimen cooled at 300 ºC/h suffered a single phase change, from austenite to martensite, which was detected between ~336 and ~160 ºC. As a result, the observed final structure was completely martensitic.

ii. Instead, cooling at 50 ºC/h resulted in two dilatometric anomalies (*FIG. 1*). The first one accounts for a transformation from austenite to ferrite (A→F), which is slow and turns out to be interrupted at that rate. In this way, a fraction of austenite is

retained and transforms to martensite (A→M) between ~410 y ~234 ºC. Thus, the resulting observed structure is mixed martensitic-ferritic.

iii. The sample cooled at 15 ºC/h displayed a phase transformation from austenite to ferrite between ~760 and ~720 ºC, resulting in a fully ferritic structure.

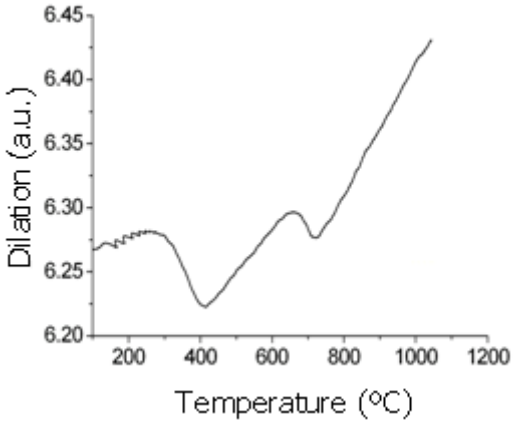


*FIG 1. Dilation as a function of temperature for the sample cooled at 50 ºC/h.*

The increment of the A→M transformation temperatures found for the 50 ºC/h cooling cycle can be attributed to changes in the composition of the austenite matrix. Indeed, the alloying element content in austenite diminishes as a consequence of the precipitation of minor phases associated to ferrite nucleation and growth, before martensite transformation. Thus, the temperature increase found is consistent with the reported increase in the martensite start temperature associated to the diminution of alloying elements such as Cr, C and N in austenite [12]. On the other hand, examples of OM images, leading to determine the ferrite percentages in mixed samples, are shown in *FIG. 2*.

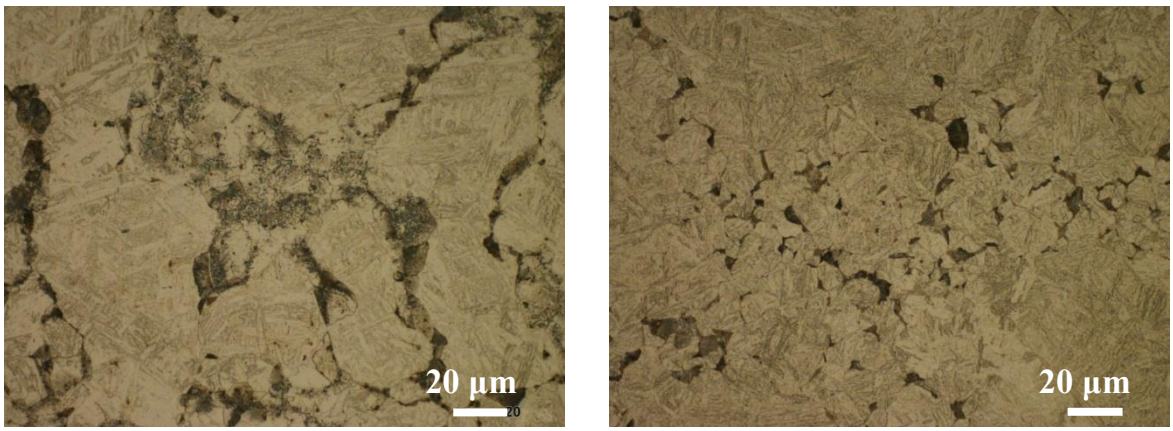


*FIG 2. Optical micrographs of the samples cooled at 50 ºC/h (left) and 100 ºC/h (right). Light zones are martensite and dark zones are ferrite + carbides.*

Ferrite percentages were evaluated to be 46 ± 2 and 2.3 ± 0.5 % for the samples cooled at 50 and 100 ºC/h respectively.

### 3.2.Field Emission Gun Scanning Electron Microscopy

*FIG: 3a*, *b* and *c* show the microstructures observed as a result of cooling at different rates.

In the case of the specimen cooled at 300 ºC/h (*FIG. 3a*), martensite laths with a few cents nanometers width are distinguished, along with minor second precipitated phases at lath boundaries and within laths.

*FIG. 3b* shows martensitic and ferritic regions corresponding to the "mixed" sample cooled at 50 ºC/h, where differences as for quantity, distribution and morphology of precipitates in both regions are apparent. On the other hand, *FIG. 3c* displays a magnified view of a ferritic region in which the orientation, size and morphology of precipitates can be appreciated.

The "mixed" structure is a consequence of the non-completion of the transformation to ferrite during cooling and, for this reason, contains information about the ferrite nucleation sites. As can be seen in optical micrographs, these sites are likely prior grain boundaries or prior triple points of the austenitic matrix, where nucleation is energetically favorable.

Finally, *FIG. 3d* corresponds to the sample cooled at 15 ºC/h, which exhibits a fully ferritic microstructure. A banded precipitation feature, which could be the result of an interphase-type precipitation mechanism during transformation from austenite to ferrite, is observed.

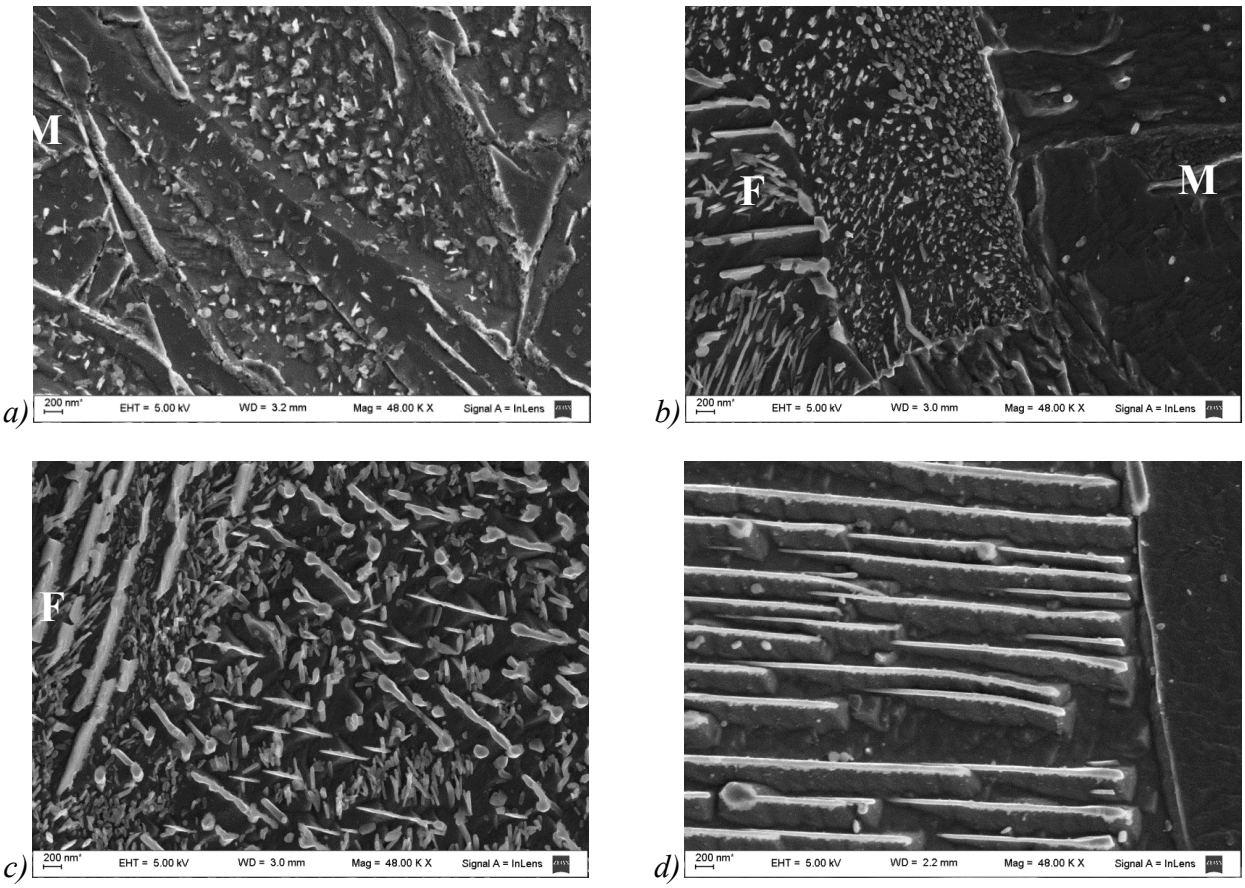


*FIG. 3: FEG-SEM micrographs of the samples cooled at 300 (a), 50 (b),(c) and 15 (d) ºC/h (48000 X). Labels (M) and (F) stand for martensitic and ferritic regions.*

### 3.3.X-Ray Diffraction

Representative angular intervals of selected X-ray spectra, fitted in accordance with the Rietveld refinement, are shown in *FIG. 4,* and the fitted parameters of the phases proposed for each sample are detailed in Table 3. The presence of retained austenite in the samples cooled at rates comprised between 300 and 50 ºC/h was determined.

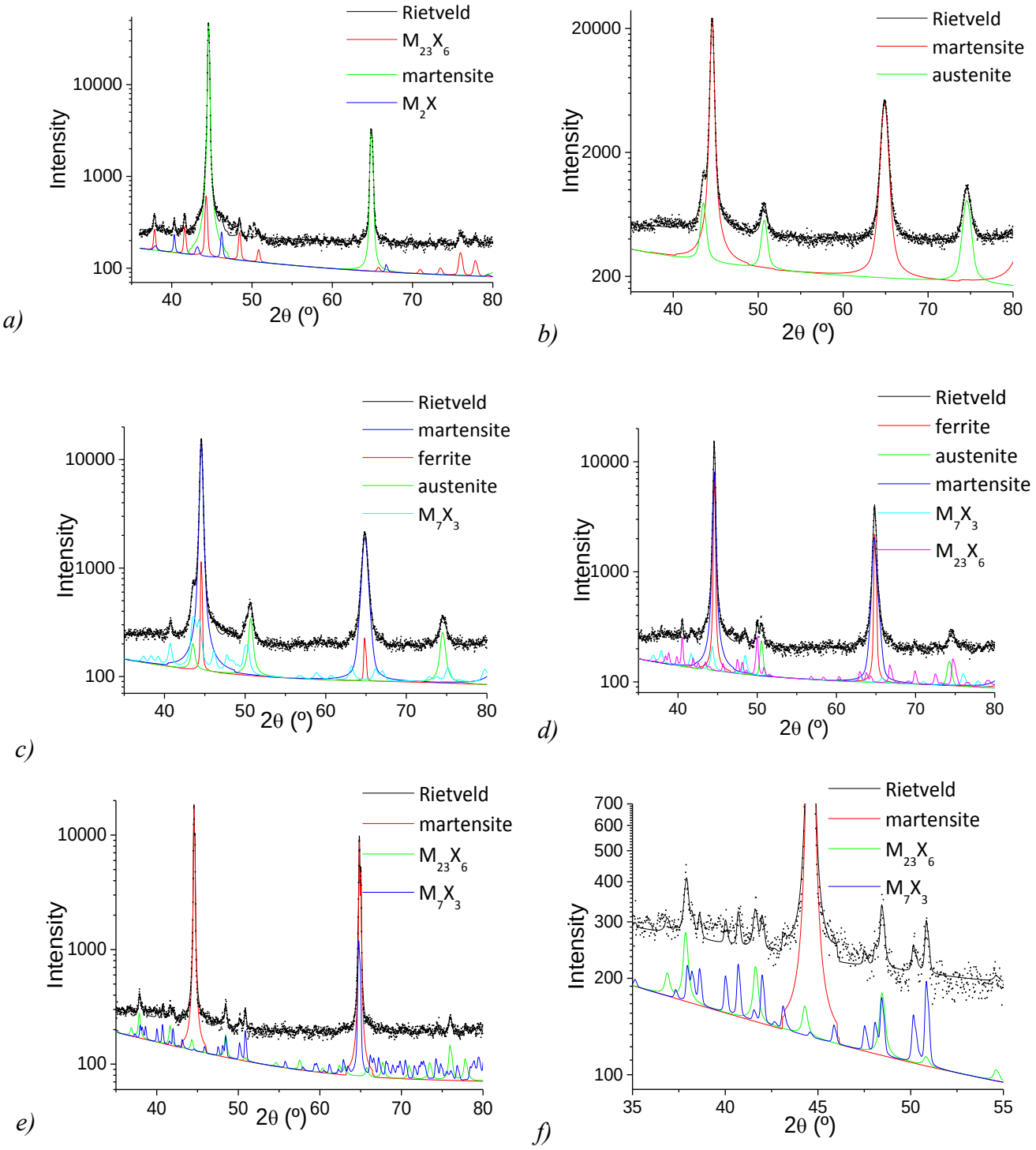


*FIG. 4: A detail of the Rietveld fitting of XRD spectra of samples: (a) As-received, and cooled at (b) 300, (c) 100, (d) 50 and (e,f) 15 ºC/h.*

TABLE 3: LATTICE PARAMETERS AND ESTIMATED VOLUME FRACTION FOR PHASES CONSIDERED IN THE RIETVELD REFINEMENT.

| **Sample** | **Phase** | **a (Å)** | **b (Å)** | **c (Å)** | **%** |
|---|---|---|---|---|---|
| As-rec. | Martensite | 2.87274 (4) | | 2.87662 (7) | 84±9 |
| | $M_{23}C_6$ | 10.630 (1) | | | 7±1.0 |
| | $M_2X$ | 4.7429(4) | | 4.468 (2) | 6±1.0 |
| 300 ºC/h | Martensite | 2.87490 (6) | | 2.8760 (1) | 92±2 |
| | Austenite | 3.6006 (3) | | | 8.0±0.1 |
| 100 ºC/h | Martensite | 2.8753 (1) | | 2.8766 (2) | 89±3 |
| | Austenite | 3.5998 (3) | | | 5.1±0.4 |
| | Ferrite | 2.8754 (1) | | | 3.2±0.1 |
| | $M_7C_3$ | 4.5078 (3) | 7.048 (1) | 12.008 (1) | 2.7±0.2 |
| 50 ºC/h | Martensite | 2.87401 (9) | | 2.8787 (1) | 45±2 |
| | Ferrite | 2.87412 (3) | | | 40±1 |
| | Austenite | 3.6120 (6) | | | 1.0±0.1 |
| | $M_{23}C_6$ | 10.626 (2) | | | 5.4±0.6 |
| | $M_7C_3$ | 4.5243 (6) | 7.089 (2) | 12.489 (2) | 4.6±0.2 |
| 15 ºC/h | Ferrite | 2.87380 (1) | | | 99.3±5 |
| | $M_{23}C_6$ | 10.625 (1) | | | 0.20±0.02 |
| | $M_7C_3$ | 4.5426 (4) | 6. 9898(6) | 12.178 (1) | 0.50±0.03 |

### 3.4.Mössbauer Spectroscopy

As an example of the procedure explained in Section 2.2, the fitting of the spectrum for the sample cooled at 50 ºC/h is presented in *FIG. 5*. Hyperfine parameters for all fittings are collected in Table 4, where δ, $2\varepsilon_Q$ and $B_{hf}$ stand for the isomer shift, quadrupolar shift and hyperfine magnetic field respectively.

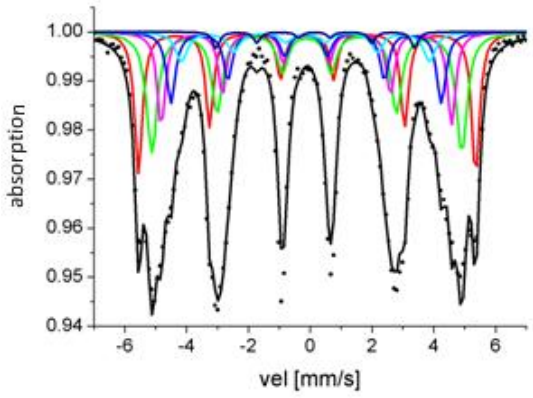


*FIG. 5: Fitting of the Mössbauer spectrum obtained for the sample cooled at 50 ºC/h.*

TABLE 4: HYPERFINE PARAMETERS AND APPROXIMATE RELATIVE PERCENTAGE CORRESPODING TO EACH CONSIDERED SUBSPECTRUM

| **Sample** | **Subespectrum** | **δ (mm/s)** | **$2\varepsilon_Q$ (mm/s)** | **$B_{hf}$ (T)** | **%** |
|---|---|---|---|---|---|
| As-Received | 1 | 0.012 | 0 | 33.99 | 21 |
| | 2 | 0.000 | 0 | 31.32 | 38 |
| | 3 | -0.011 | 0 | 29.40 | 17 |
| | 4 | -0.023 | 0 | 27.07 | 17 |
| | 5 | -0.025 | 0 | 24.84 | 6 |
| | 6 | 0.259 | 0.03 | 19.93 | 1 |
| 300 ºC/h | 1 | 0.012 | 0 | 33.98 | 18 |
| | 2 | 0.007 | 0 | 31.30 | 31 |
| | 3 | -0.002 | 0 | 29.23 | 21 |
| | 4 | -0.017 | 0 | 26.95 | 18 |
| | 5 | -0.018 | 0 | 24.95 | 10 |
| | 6 | 0.260 | 0.03 | 19.93 | 2 |
| 100 ºC/h | 1 | 0.013 | 0 | 33.84 | 19 |
| | 2 | -0.002 | 0 | 31.10 | 34 |
| | 3 | -0.003 | 0 | 29.13 | 17 |
| | 4 | -0.017 | 0 | 27.19 | 14 |
| | 5 | -0.017 | 0 | 25.03 | 13 |
| | 6 | 0.264 | 0.03 | 20.12 | 3 |
| 50 ºC/h | 1 | 0.008 | 0 | 33.83 | 22 |
| | 2 | -0.001 | 0 | 31.09 | 36 |
| | 3 | -0.013 | 0 | 29.13 | 16 |
| | 4 | -0.021 | 0 | 27.13 | 14 |
| | 5 | -0.043 | 0 | 24.91 | 10 |
| | 6 | 0.260 | 0.03 | 19.91 | 2 |
| 15 ºC/h | 1 | 0.005 | 0 | 33.49 | 28 |
| | 2 | -0.004 | 0 | 30.83 | 32 |
| | 3 | -0.020 | 0 | 28.96 | 17 |
| | 4 | -0.025 | 0 | 27.12 | 13 |
| | 5 | -0.075 | 0 | 25.23 | 8 |
| | 6 | 0.261 | 0.03 | 20.21 | 2 |

## 4. Conclusions

- Fully martensitic and fully ferritic structures were observed as a result of cooling at 300 and 15 ºC/h, respectively. Intermediate cooling rates −100 and 50 ºC/h− gave final "mixed" martensitic-ferritic microstructures, with ferrite phase percentages of 2.3 ± 0.5 and 46±2% respectively. The values for martensite and ferrite critical cooling rates were bounded within the intervals 200-140 ºC/h and 25-15 ºC/h respectively.
- Retained austenite was observed to be present for the samples cooled at rates comprised between 300 and 50 ºC/h. Precipitated second phases with different morphologies and nucleation sites, either in grain boundaries or within grains, were also observed. From X-ray analysis, the possibility of presence of the minor phases $M_{23}X_6$ and/or $M_7X_3$ is hypothesized for the samples cooled at 100, 50 and 15 ºC/h.
- Mössbauer spectra indicated the existence of different surroundings for iron atoms in the bcc matrix and an additional contribution that would correspond to the cementite alloyed ($(Fe,Cr)_3C$) phase. This cementite contribution was present in all of the analyzed samples.

## 5. References

[1] HAARMAN, K., VAILLANT, J.C., The T91/P91 Book, second ed., Vallourec & Mannesmann Tubes, Düsseldorf, 2002.

[2] SASAKI, T., et al., "Production and properties of seamless modified 9Cr-1Mo steel boiler tubes", Kawasaki Steel Tech. Rep. 25 (1991) 78.

[3] BÉRES, L., et al., "Welding of martensitic creep resistant steels", Weld. Res. Supp. (2001) 191s.

[4] TAMURA, M., et al., "A new approach to improve creep resistance of high Cr martensitic steel", J. Nuc. Mater. **417** (2011) 29.

[5] PLESIUTSCHNIG, E., et al., "Ferritic phase transformation to improve creep properties of martensitic high Cr steels", Scr. Mater. **122** (2016) 98.

[6] OHGAMI, M., et al., "Development of 9CrW tube, pipe and forging for ultra supercritical power plant boilers", Nippon Steel Technical Report Nº 72, 1997.

[7] LUTTEROTTI, L., et al., "MAUD: a friendly Java program for material analysis using diffraction", IUCr Newsletter of the CPD **21** (1999) 14.

[8] POPA, N.C., "The (hkl) dependence of diffraction-line broadening caused by strain and size for all Laue groups in Rietveld refinement", J. Appl. Crystallogr. **31** (1998) 176.

[9] CAGLIOTI, G., et al., "Choice of collimator for a crystal spectrometer for neutron diffraction", Nucl. Instrum. **3** (1958) 223.

[10] ENG-POH, Ng, et al., "Capturing Ultrasmall EMT Zeolite from Template-Free Systems", Science **335** (2012 ) 70.

[11] BRAND, R.A., Normos program, Internat. Rep. Angewandte Physic, Duisburg University, 1987.

[12] BRACHET, J.C., "Correlation between thermoelectric power (TEP) and martensite start temperature ($M_s$) measurements of 9Cr-W-V-(Ta) martensitic steels", J. Phys. IV Colloque **05** (1995), C8 339.